Available online at www.sciencedirect.com
ScienceDirect
Trans. Nonferrous Met. Soc. China 34(2024) 2095−2107
Transactions of Nonferrous Metals Society of China
www.tnmsc.cn

In situ observation of multi-grain competitive growth in Al−20wt.%Cu and establishment of converging-case dendrite elimination model

Fa-guo LI[1], Lian ZHOU[1], Yu XIE[2], Jiao ZHANG[3], Mike DODGE[4], Fu-cheng YIN[1], Bao-de SUN[3]

1. Key Laboratory of Materials Design and Preparation Technology of Hunan Province, School of Materials Science and Engineering, Xiangtan University, Xiangtan 411105, China;
2. Central Research Institute, Baoshan Iron & Steel Co., Ltd., Shanghai 201900, China;
3. School of Materials Science and Engineering, Shanghai Jiao Tong University, Shanghai 200240, China;
4. TWI Ltd, Granta Park, Great Abington, Cambridge CB21 6AL, UK

Received 8 January 2023; accepted 19 September 2023

Abstract: Synchrotron radiography was performed during the solidification of Al−20wt.%Cu hypoeutectic alloy to study the competitive grain growth dynamics and a mathematical model consistent with the experimental results was established. The experimental results showed that for the diverging competitive growth, the "normal elimination" rule played a role. For converging competitive growth, the growth rate of the primary dendrite arms in the non-preferentially oriented grains was accelerated due to constitutional supercooling, resulting in the phenomenon of "abnormal elimination" in which the non-preferentially oriented dendrites would eliminate the preferentially oriented dendrites. The critical conditions between "normal elimination" and "abnormal elimination" of converging competitive growth were explored using a mathematical model. The mathematical model named the "secondary dendrite arm blocking model" among dendrite growth rate, dendrite arm spacing and dendrite inclination angle was established, which could quickly predict the orientation of grain boundaries and the type of elimination.

Key words: competitive growth; synchrotron radiography; directional solidification; mathematical model; Al−Cu alloys

1 Introduction

Single crystal nickel-alloy turbine blades are commonly used in aero-engines and gas turbines where the ⟨001⟩ growth direction has a relatively low elastic modulus, high temperature creep and fatigue resistance [1,2]. In order to ensure that the crystal grows in the ⟨001⟩ direction, a grain selection method or "seeding grain" method was generally used to control growth orientation [3,4]. These methods promoted competitive growth among various grain directions during initial solidification so that unfavorable orientations were eliminated in the finished component [5].

WALTON and CHALMERS [6] first proposed a model for two-dimensional (2D) bi-crystal competitive growth, i.e. the W−C model. The competitive growth between an unfavorably orientated (UO) grain and a favorably orientated (FO) grain was studied. The FO grain has a lower inclination angle (θ) than the UO grain. Converging and diverging competitive growth, forming the converging and diverging grain boundaries (GBs), respectively, are considered in the model by assuming that the growth rates of Dendrite 1 (θ_1) and

Corresponding author: Fa-guo LI, Tel: +86-731-58298235, E-mail: lifaguo@xtu.edu.cn;
Yu XIE, Tel: +86-21-26643924, E-mail: xieyu@baosteel.com
DOI: 10.1016/S1003-6326(24)66527-1

Dendrite 2 (θ_2) are V_1 and V_2:

$$\frac{V_1}{V_2}=\frac{\cos\theta_2}{\cos\theta_1}=f_{\mathrm{W-C}}(\theta_1,\theta_2)<1 \tag{1}$$

As predicted in Eq. (1), the FO dendrite with faster growth velocity survives whether under converging or diverging growth conditions. This is known as the rule of "survival of the fittest", as proposed in the W−C model for the competitive growth.

The W−C model is relatively simple, as it does not consider that the growth rate and inclination angle may vary with time, and the solute interactions between grains. With the consideration of solute interactions around GBs, UO grains overgrowing FO grains in the converging case are predicted because of the linear increase in GB angle [7]. The evolution of diverging GBs during competitive growth is strongly affected by the inclination angles while converging GBs exhibit a lower dependence on the inclination angles [8]. Compared to the 2D multi-grain growth, dendrite insertion with dendrite spacing adjustment and lateral motion of non-uniplanar GBs usually happen in 3D cases [9,10]. The competitive growth of grains and the migration of GBs are mutually influenced [11]. As a result, the FO grain overgrows the UO grain due to the development of the new dendrites in the lateral gap [9].

For diverging competitive growth, all diverging GB degrees are the averages of the two grain growth degrees [12]. The choice of diverging GB trajectories is random because of the inherent randomness of side branches and the chaotic dynamics of subsequent branch competition [13]. Moreover, studies have shown that the secondary arm spacings and the distance between the primary dendrite tip and the tertiary dendrite tip play a dominant role in GB orientation selection [14]. The occupation of the interstitial region between two diverging grains by FO grains is mainly determined by the growth direction difference of the secondary dendrite arms of FO grain and UO grain [15]. In addition, columnar-to-equiaxed transition (CET), which should be prevented in the directional solidification of single crystals, may happen because of the increased likelihood of dendrite fragmentation in the solute-rich regions around the diverging GBs [16].

For the converging GBs, the dendrites overgrow the eliminated ones either by generating new primary arm dendrites through tertiary branching or by the growth of the existing primary dendrite arms, depending on the misorientation arrangement between these two morphologies [17]. Phase-field simulation results show there exists a critical misorientation difference to decide whether FO or UO overgrows one another [18]. At the critical misorientation difference, the FO dendrites and UO dendrites can coexist, and growth selection does not happen [19].

Recently, with synchrotron radiation imaging technology, researchers can accurately and quantitatively describe dendrite growth in a more detailed manner [20,21]. In this work, to study competitive growth in multi-grain systems under the directional solidification conditions, the synchrotron radiation imaging technique was used. A hypoeutectic Al−Cu alloy was selected as the experimental object because it is able to form well-developed dendrites with a wide solidification temperature range [22]. Based on the experimental results, the competitive growth mechanism of directional solidification was discussed and a general model to predict the results of competitive growth was proposed.

2 Experimental

A vacuum resistance furnace with dual temperature zone and the power down method were used to carry out the directional solidification. To ensure that the X-ray passes through the sample and is received by the CCD, the vacuum resistance furnace had optical windows in two opposite faces, as shown in Fig. 1. The Al−20wt.%Cu alloy used in the experiment was smelted from high-purity aluminum (99.999 wt.%) and high-purity copper (99.9999 wt.%). The sample used in this experiment was 0.5 mm in thickness, 50 mm in length and 20 mm in width. It was polished and enclosed between two Al_2O_3 plates with a thickness of 150 μm. Directional solidification experiments were carried out on BL13WB1 of Shanghai Synchrotron Radiation Facility (SSRF), Shanghai, China [23]. The temperature gradient (G_T) and the cooling rate (R_T) of the directional solidification set in the experiments are listed in Table 1.

The X-ray absorption contrast imaging principle was applied to obtaining the sequence of

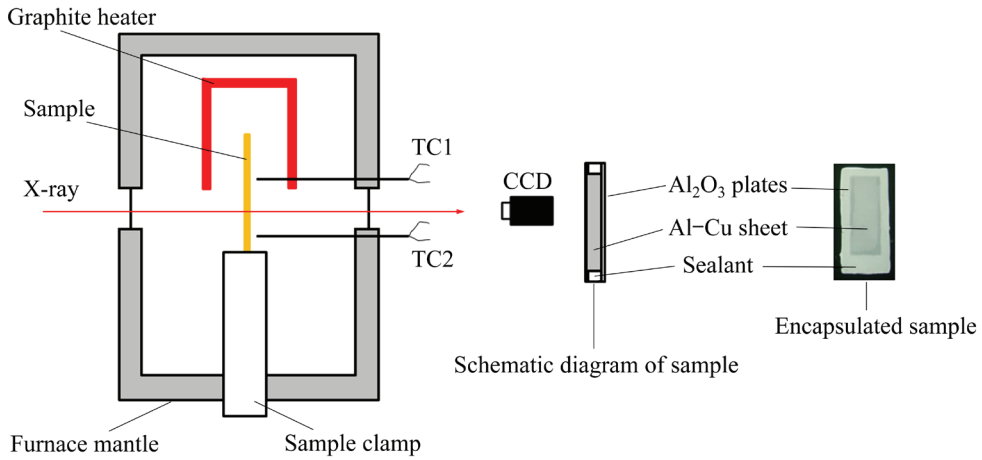

Fig. 1 Schematic of experimental setup, including heating furnace and sample

Table 1 Experimental parameters

Experimental parameter	Value
Temperature gradient, G_T/(K·cm^{-1})	42
Cooling rate, R_T/(K·min^{-1})	30
Incident monochromatic X-ray energy/keV	26
Image spatial resolution	7.4 μm × 7.4 μm per pixel
Time interval between images/s	0.5
Field of view/μm^2	7562.8 (width) × 4121.8 (height)

images, in which the brightness of each pixel was inversely proportional to the concentration of the Cu solute [24]. Here, the angle inclined to the left was defined as positive and otherwise negative. The length of the dendrite arm was measured by Image-pro 6.0 software and the measurement error was within 5%.

3 Results and discussion

3.1 Competitive growth of multiple grains with same inclination direction

Figure 2 shows a sequence of images indicating competitive growth between multiple grains inclined to the same direction. The α(Al) dendrite lack of Cu solute appears as white and branch-like while the inter-dendrite regions that are rich in Cu solute appear darker. A yellow dashed line is drawn to show the wavy distribution of Cu solute at the front of the solid−liquid interface in Fig. 2. The dendrite growth here can be considered as confined growth. The thickness of the sample is 0.5 mm and the thermal diffusivity of the liquid of Al−20wt.%Cu is in the order of 10^{-5} m^2/s. Then, the temperature gradient distributing along the thickness direction by the thermal diffusion is as small as 10^{-3} K/mm, almost equal to zero. Under such a temperature gradient along the thickness direction, it is hard for the solid to grow along the thickness direction, and the dendrite growth is limited in pseudo-two-dimensional plane. Only the upward-growing primary dendrite arm is likely to grow continuously, which is equivalent to limiting the forward, backward and downward growth. This growth of dendrites in a "crystal selector"-liker minimizes projection errors. For easy discussion, the grains with primary dendrite and higher order of dendrite arms is symbolized in a form of Capital letter with number connecting higher order (number in subscript means the order) of dendrite arms with the symbol of "_". For instance, E1 means the 1$^{\#}$ primary dendrite of Grain E, and E1_1$_2$ means the 1$^{\#}$ secondary dendrite arm of the 1$^{\#}$ primary dendrite.

The starting point of competitive growth is 2.5 s (Fig. 2(a)), where the inclination angles (θ) of Grains A, B, C and E are 35°, 14°, 21° and 47°, respectively. In this image, Grains A and B demonstrate the diverging growth case where Grain A is the UO grain and Grain B is the FO grain. For the diverging case, as pointed out in the previous studies [8−10], the average grain boundary orientation almost kept constant although the trajectories of the diverging GB fluctuated. New dendrites would develop to fill the diverging

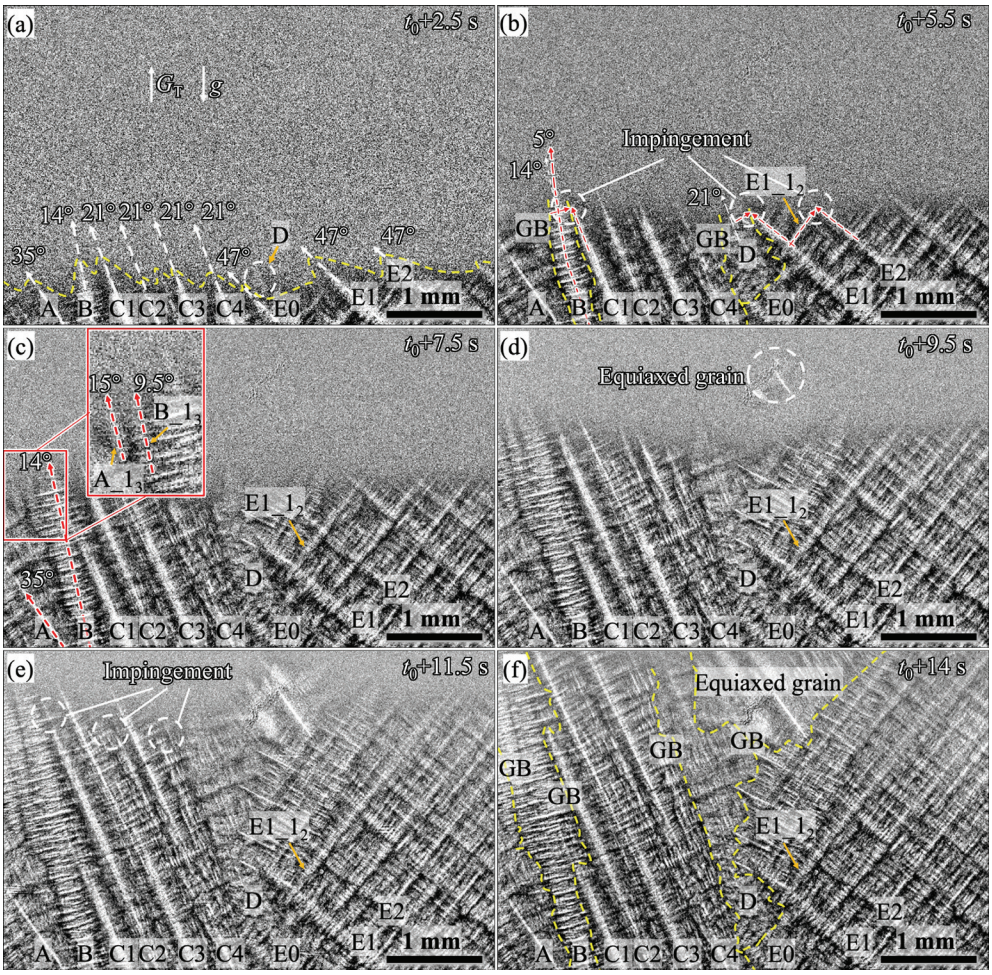

Fig. 2 Sequence of images showing competitive growth of multiple grains inclined to same direction in Al−20wt.%Cu sample (G_T−Temperature gradient; g−Gravity)

gap [25]. During the development of the new dendrite, the growth of secondary arms behind the primary dendrite tip was controlled by cooperative growth between Grain A and Grain B (Fig. 2(a)). Once the undercooling driving the growth increased to some extent due to the cooperative growth, one side arm could escape from the control of cooperative growth and grow into an extended side branch, as shown in Fig. 2(b) captured at t_0+5.5 s.

An interesting phenomenon emerged during competitive growth between Grains A and B. As shown in Fig. 2(c), two new inclination tertiary dendrite arms denoted as A_1$_3$ and B_1$_3$ grew out at the diverging GB. Although the inclination angle of tertiary dendrite A_1$_3$ of 15° was larger than that of tertiary dendrite B_1$_3$ (9.5°), tertiary dendrite A_1$_3$ and tertiary dendrite B_1$_3$ could grow side by side probably because the inclination angle of A_1$_3$ was very close to that of FO grain B (14°). The growth of the A_1$_3$ and B_1$_3$ would change the trend of the original grain boundary between Grain A and Grain B. As a result, the UO grain (Grain A) would not be eliminated by the FO grain (Grain B), which deviated from the W−C model. Although the crystal orientation of the side branches was the same as that of the primary dendrite, unlike the primary dendrite, the growth direction of side branches was mainly susceptible to the influence of temperature field and flow field, which was influenced by the solute grooves among diverging grains. Solute grooves formed among diverging grains bring thermal mass flow due to local solute deposition, causing side branch inclination [26]. The random change of the inclination angle of the tertiary dendrite induced by the solute field made competitive grain growth complicated, leading to the UO grain surviving as observed. Furthermore, the root of the tertiary dendrite A_1$_3$ showed an

obvious necking phenomenon, and the tertiary dendrite deformed and bend with the narrowing of the neck. Therefore, the uncertainty of side branch growth caused by local environmental conditions increased the complexity of diverging competitive growth and probably led to the deviation of the W−C model.

Grains B and Grain C exemplified the converging case, where Grain B was the FO grain and Grain C was the UO grain. As shown in Fig. 2(b), the FO dendrite B bent and deflected in the direction parallel to heat flow, and the inclination angle (θ) became 5° from the original 14°. The UO dendrite C1 (primary dendrite) adjacent to Grain B was blocked by the secondary dendrite arm near the tip of Dendrite B, in accordance with the W−C model. An observation of a complex case that cannot be predicted by the W−C model is shown in Fig. 2(e), in which the primary dendrites (Dendrites C1−C4) of a nearby grain joined the competitive growth process. As shown in Fig. 2(e), there existed conditions of competitive growth between Dendrites B and C1, where Dendrite B was blocked by C2. Meanwhile, the two adjacent dendrites of a grain competed during growth and adjusted the primary arm spacing of the grain. Before t_0+5.5 s, the primary dendrite arm spacing of Grain C was about 348 μm by measurement. As the dendrites continued to grow, the primary dendrite arm spacing between C3 and C4 increased to 430 μm, which led to the phenomenon of tertiary dendrite arm competition to regulate the primary dendritic arm spacing [25]. The developed tertiary dendrite arm of C3 reduced the excessive primary dendritic arm spacing, and the tertiary dendrite arm was blocked by the second dendrite arm.

The Grain C and Grain E were also converging grains, where Grain C represented the FO grain, and Grain E was the UO grain. Grain E comprised three primary dendrites (Dendrites E0−E2) with the same inclination direction, as shown in Fig. 2(a). The left inclination angle of the primary dendrite arm of Grain E entering the field of view was larger than 45°, indicating that there was also a primary dendrite arm that tilted to the right outside the field of view, and the inclination angle was less than 45°. The angle between them was 90°, one tilted to the left, and the other tilted to the right, diverging growth. However, the secondary dendrite arms grown from the primary dendrite arms (Grain E in the field of view) with an inclination angle larger than 45° must have an inclination angle less than 45°, thus preventing the growth of adjacent primary dendrite arms (or tertiary dendrite arms). When the inclination angle of Dendrite E0 exceeded 45°, a solute-enriched boundary layer was generated at the growth front of E0. When the solute-enriched boundary layer of E0 met the solute boundary layer of the adjacent dendrite, C4, the growth rate of E0 slowed down due to lower undercooling. Such local dendrite growth was slow and solute enrichment effect could easily induce high-order dendrite arm remelting and fracture, forming dendrite fragments [27]. Figure 2(b) shows that the secondary dendrite arm near the dendrite tip of Dendrite E0 was broken and a new grain D was formed. Due to the formation of the new grain, direct competition between Grains C and E ceases, and is replaced by competitive growth between new grain (i.e., C vs D and D vs E). In this case, the inclination angle between grains C and D differs whereas it is the same between Grains D and E.

With solidification proceeding, the E0 dendrite stopped growing due to the “self-poisoning” effect, as shown in Fig. 2(b). The UO dendrite E1 was also blocked by the newly dendrite D, which was the same as W−C model. Since the inclination angle of grain E was larger than 45°, the secondary dendrite arms were the FO dendrites compared with the primary dendrite arm. Then, the primary dendrite arm of Dendrite E2 was overgrown by the secondary dendrite arm of Dendrite E1, as shown in Fig. 2(b). When converging primary dendrites were stunted, the secondary dendrite arms would act as the primary dendrites and became the diverging growth, as observed between Grains D and E. As a result, Grain E changed from a left tilted growth to right tilted growth and converted the converging case between Grain D and Grain E to the diverging case, which is the so-called converging-to-diverging transition (CDT).

With competitive growth proceeding between Grain D and Grain E shown in Fig. 2(d) after the CDT, new secondary and tertiary dendrite arms were grown out between the diverging Grain D and Grain E to fill the gaps, resulting in tortuous grain boundaries. The front of diverging grains would form a very wide solute groove, and the existence of this solute groove was likely to induce the

columnar-to-equiaxed transition (CET) [16]. The CET during the competitive growth tend to happen after the dendrite fragment which is the result of the dendrite remelting, detachment and floating of the dendrite fragments led by the dendrite necklace in the solute groove [28]. The fragment part would be a nucleation of the new equiaxed grains. As shown in Fig. 2(d), the spontaneous nucleation of an equiaxed grain appeared at a diverging groove. It is expected that the equiaxed grain can continue to grow into columnar grain, but this CET-like phenomenon can disrupt the continuity of directional growth.

From the above observations, the solute interaction between side branches and dendrites in experiments makes the process more complicated than that in the W−C model. In this experiment, UO grain A survives in the competitive growth against the FO grain B because of the formation of the tertiary arms. Transformation from the converging case to the diverging case was found to occur during competitive growth between Grain E and the newly formed Grain D, as well as the CET phenomenon. Therefore, the influence of the high-order dendrites at the grain boundaries on competitive growth cannot be neglected in the competitive growth of multiple grains with the same inclination direction.

3.2 Competitive growth of multiple grains with different inclination directions

Figure 3 shows the competitive growth process of three grains with different inclination directions, in which Grain F and Grain G exhibit the converging case while Grain G and Grain H are in the diverging case. In the converging case, Grain F was the FO grain. As shown in Figs. 3(c, d), Dendrite G was blocked by the secondary dendrite arms of Dendrite F4 and the tertiary dendrite G_1_3 was blocked by the tertiary dendrite F4_1_3 at the GB. The dendrites of the UO grains G were eliminated by the FO grains F, resulting in the

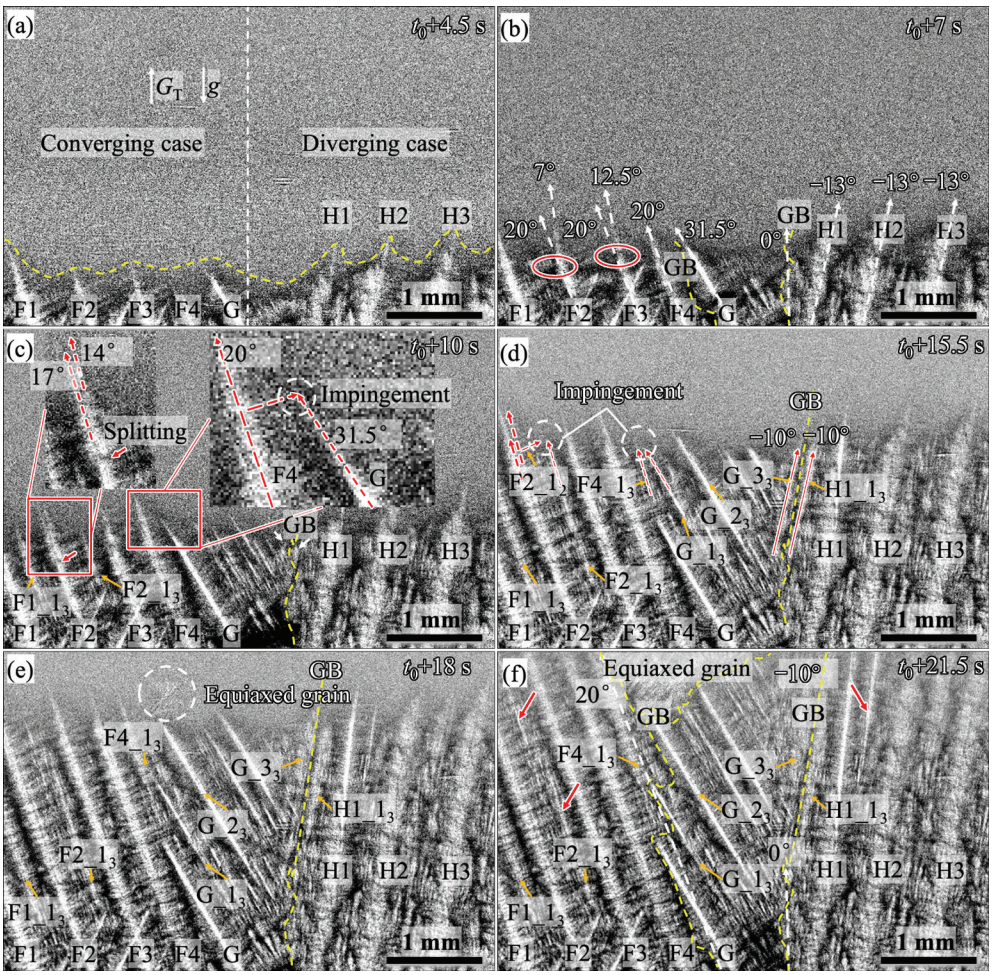

Fig. 3 Sequence of images showing competitive growth of multiple grains inclined to different directions in Al−20wt.%Cu sample

formation of the GB along the growth direction of the FO grains F. The growth of the secondary dendrite arm would decrease the speed of its primary arm, and other dendrites of Grain G would overgrow the FO grain, as shown in Fig. 3(f). As a result, the FO grains would be gradually occupied by the UO grains G via "survival of the inferior" phenomenon. The key to avoiding the "survival of the inferior" phenomenon was that the side branches of the FO grain must grow fast enough to block the primary dendrite arms of the UO grain and occupied the UO grain area.

Since the G grains lagged behind the F grains, a concave groove was formed between them, cultivating a favored environment for the growing out of new equiaxed grains that completely blocked the G grains from growing (Figs. 3(e–f)). In the converging case, equiaxed grains then spontaneously nucleated at the dendrite growth front. Although this was observed in the divergent case in previous study [16] and as well observed in our experiment in diverging case (Fig. 3(d)) as discussed earlier, it was rarely reported in the converging case. Once the initiation of the equiaxed grains, the development of the equiaxed grains in front of the dendrite growth tended to block the growth of the nearby directional grains.

Moreover, the dendrite tips of primary dendrite F2 and primary dendrite F3 were bent due to the extrusion of the adjacent secondary dendrite arm tips, and the inclination angle changed (7°, 12.5°), as indicated by the solid red ellipse (Fig. 3(b)). No dendrite separation occurred, and the inclination angle was back to a certain extent, as shown in Fig. 3(c). However, as shown in the enlarged view of Fig. 3(c), there were obvious tip splitting. Tip bifurcation occurred, resulting in two dendrite tips. Dendrite bending can change the growth direction, but the dendrite can bifurcate from the bend, and the two dendrite tips can grow close to the original growth direction. Tertiary dendrite arms blocked by adjacent secondary dendrite arms cannot develop into new "primary dendrite arms". However, an interesting phenomenon was observed different from the previous one. The primary dendrite arm spacings of Grain F from Dendrites F1−F4 were 555, 555 and 333 μm, respectively, as shown in Fig. 3(c). When the distance between the primary dendrite arms was too large, the tertiary dendrite arms F1_1_3 and F2_1_3 developed and played a role in regulating the primary dendrite arm spacing. At the same time, there was a competitive relationship between the tertiary dendrite arm and the secondary dendrite arm of the grain. As shown in Fig. 3(d), the tertiary dendrite arm, F2_1_3, was blocked by the secondary dendrite arm, F2_1_2, and stopped growing. Although the tertiary dendritic arm, F2_1_3, was eliminated, a new tertiary dendrite arm would be soon formed on F2_1_2 and developed into a "primary dendrite arm" to reduce the primary dendrite arm spacing (Fig. 3(f)).

As shown in Fig. 3(b), the GB orientation between diverging grains G and H fluctuated along the 0° direction, which accorded with the simulation results of GUO et al [15] reporting that the absolute value of the grain inclination in the range of 30°−35° keeps the GB angle at 0°. These two grains generated two side branches with an inclination angle of 10° at the GB, denoted as G_3_3 (tertiary dendrite) and H1_1_3 (tertiary dendrite), as shown in Fig. 3(d). The competitive growth between Grains G and H changed from the diverging case shown in Fig. 3(a) to the converging case shown in Fig. 3(d). This phenomenon of "diverging to converging transition" (DCT) was opposite to the CDT phenomenon previously described. Figure 3(d) showed that the convergence of grains G and H was achieved only by tertiary dendrite G_3_3. In fact, the other primary dendrite arms in Grain G remained in a diverging state with Grain H. A diverging situation was formed between tertiary dendrite G_3_3 and other primary dendrite arms of Grain G. Of course, this "diverging case" behavior inside Grain G favored its own spatial expansion. It was foreseeable that the G grains could continue to occupy the space of F grains, forming a competitive growth result via "survival of the inferior".

As discussed above, the phenomenon of secondary dendrite arms blocking the adjacent primary dendrite arms was a commonly observed phenomenon. On this basis, it would be advantageous to derive a description of a "secondary arm blocking model" for cases of converging competitive growth.

3.3 Evolution of dendrite growth rate during competitive growth

Competitive grain growth was ultimately determined by the movement of grain boundaries,

but it was undeniable that the competition among side-dendrites at grain boundaries was the main factor governing the competitive process. The inclination angle and growth rate of dendrites (measured in the dendrite arm directions) were two key parameters for the competitive growth.

Although it was not observed in the experiment, a situation could happen during the competitive growth: A primary dendrite tip would hit the wall and stop growing, but a secondary arm would develop in the thickness direction where a tertiary arm grew out and led to a sudden interruption of the primary dendrite tip growth. The time interval of the images taken in synchrotron radiation imaging experiment was 0.5 s. The growth rate of dendrites was calculated by measuring the length of relevant dendrites in each image in time order to obtain the relationship between length and time. Figure 4 shows the curve of dendrite length versus time. As the relationship between dendrite length and time is almost a straight line, the dendrites in the field of view were in an almost stable directional solidification process where the dendrite growth rate rarely fluctuated.

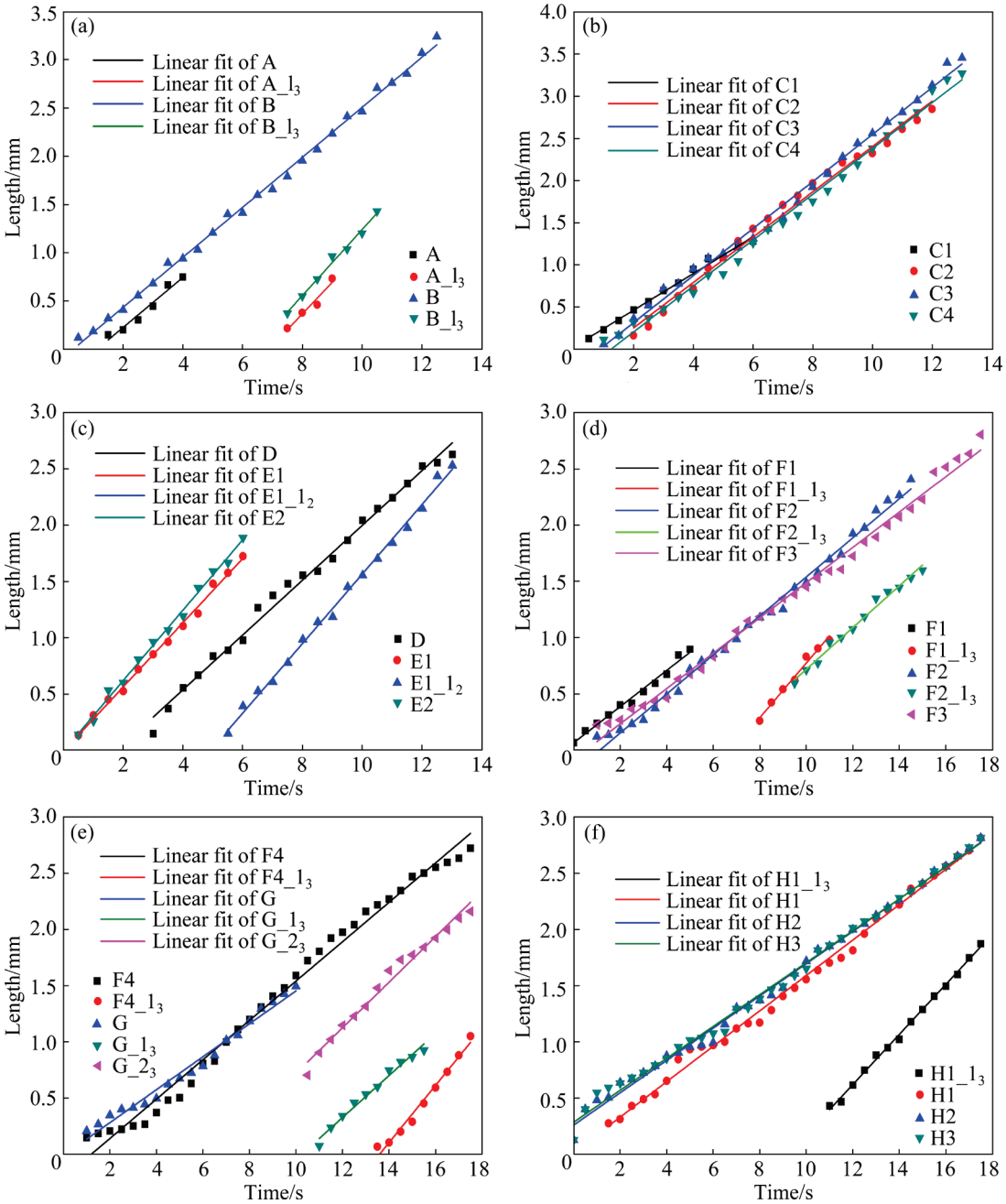

Fig. 4 Graphical relationship between dendrite length and time

In Table 2, the growth rate of primary dendrite arms among grains with different inclination angles did not strictly follow the theoretical model shown in Eq. (1), but smaller than that calculated by the W−C model according to the degrees and the growth rate of Dendrite B, attributed to the solute rich-redistributed by the growth of the secondary dendrite arms on Dendrite B. As for competitive growth among dendrites in one grain, the average growth rate of dendrites at the FO grain boundary was larger than that of dendrites at the UO grain boundary, attributed to the phenomenon of self-poisoning [29].

When tertiary arms grew outwards, the growth rate of the tertiary dendrite arm developed within each dendrite was greater than that of the primary dendrite arm. This occurred because the tip of the newly developed tertiary dendrite arm lagged far behind the primary dendrite arm and was in a state of large undercooling. With the continuous growth, the advantage of high-order dendrites in velocity would block the low-order dendrites. When the growth rate of converging FO dendrites in the same inclination direction was larger than that of UO dendrites, concave grooves would be formed at the growth front, probably leading to the nucleation of equiaxed grains.

4 Establishment of model to describe competitive growth with side branches

So far, the models to predict competitive growth results have been based on the relationship between dendrite inclination angle and grain boundary angle, as that in the W−C model [6], temperature field (TF) model [30], solute field (SF) model [7], TF-SF model [19]. PINEAU et al [31] used the phase-field method to discuss the competition between primary dendrite arms at various inclination angles and gave a complete grain boundary orientation map. In the model, the relation between the inclination angle of primary dendrite arms and the inclination angle of grain boundaries was established. These models were limited to predict the outcome of simple multi-grain competitive growth by neglecting the factors relating to the growth out of side branches, and only putting the angles as the input parameters. However, as shown by the in-situ experiments above, side branches have key roles in determining the competitive growth. Furthermore, DORARI et al [14] studied the effect of growth rate and the dendrite arm spacing to build a predictive model, which inspires us to build a model related to the characteristic parameters of dendrites to predict the competitive growth of various grains in practical production.

The model proposed is expected to describe the competitive growth of large-scale grains considering the influence of side branches by studying the phenomenon that high-order dendrite arms block low-order dendrites during the competitive growth, as referred to “secondary dendrite arm blocking” model (SDAB model for short). The SDAB model considered the inclination, the dendrite growth rate, the dendrite arm spacing and the time at which the collision of dendrite tips occurred. Since large-scale solute segregation and dendrite drift due to the liquid flow were not observed in the experiment, no obvious liquid convection happened in a macroscopic scale and the temperature and solute field had a determinant effect on the dendritic growth. From the micrometer scale, liquid flow would lead to the fluctuation in the velocity which might decrease the accuracy of the mathematical model. From the results of the calculation of the growth rate of the primary/branch arming tip, the velocity is almost constant. Therefore, the mathematical model proposed based on the constant velocity cannot cover the case in which liquid flow has a stronger effect on the growth.

FO grains exhibit abnormal overgrowth in the converging case while diverging case tends to follow the W−C model of “survival of the fittest” although dynamic processes are more complex [7].

Table 2 Average growth rates of dendrites shown in Figs. 2 and 3 (μm/s)

A	A_1_3	B	B_1_3	C1	C2	C3	C4	D	E1	$E1\_1_2$	E2
259	327	259	342	217	217	279	272	243	285	309	313
F1	$F1\_1_3$	F2	$F2\_1_3$	F3	F4	$F4\_1_3$	G	G_1_3	G_2_3	$H1\_1_3$	H1	H2	H3
161	243	174	186	157	175	255	147	187	203	223	157	144	142

The converging growth in which the competitive growth of dendrites occurs, is discussed, with an attempt to address abnormal competitive growth. Two dendrites with the same inclination direction as a general case, are shown in Fig. 5.

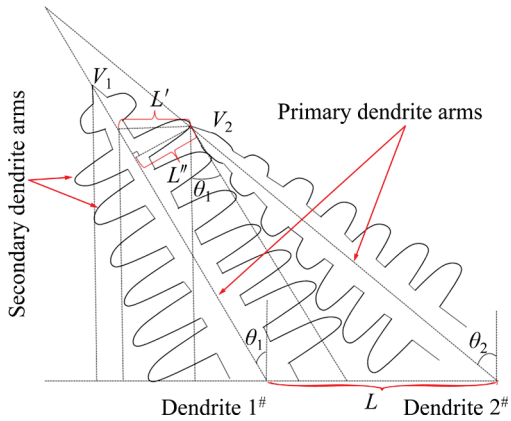

Fig. 5 Schematic diagram of "secondary dendrite arm blocking model" with arbitrary inclination angles

Two assumptions, which are in accordance with the experimental observations, are made in the model. First, there is enough space between FO dendrites and UO dendrites to allow the growth of secondary dendrite arms, assuming that the distance between FO dendrites and UO dendrites is $L\geq\lambda_1$; This assumption is in an agreement with the experimental observations, indicating that the initial spacing of the two grains is larger than the primary dendrite arm spacing, as shown in Figs. 2(a) and 3(a). Second, the growth of FO dendrites and UO dendrites is affected by the secondary dendrite arms between the two dendrites. There is enough space to grow secondary dendrite arms in preference to the UO dendrites, and the secondary dendrite arms near the tip of FO dendrites block the growth of UO dendrites.

According to the assumptions, the schematic diagram of the model are shown in Fig. 5, in which the secondary dendrite arms near the tip of FO dendrite block the growth of UO dendrites. The growth rates of the primary arm are V_1 and V_2, and the inclination angles of the two dendrites are denoted as θ_1 and θ_2 satisfying the condition that $0\leq\theta_1\leq\theta_2\leq45°$. The horizontal distance between two dendrites is L, and λ_1 is the primary arm spacing. The critical condition is the contact between the secondary dendrite tip near the FO dendrite tip and the UO primary dendrite arm tip. Assuming that L' is the horizontal distance from the tip of the UO dendrite to the FO dendrite, then L' can be expressed as

$$L'=L-(V_2\sin\theta_2-V_2\cos\theta_2\cdot\tan\theta_1)t \tag{2}$$

where t is the time where the secondary dendrite of FO grain just blocks the primary dendrite of the UO grain. The secondary dendrite length when blocking UO dendrites is

$$L''=L'\sin\left(\frac{\pi}{2}-\theta_1\right)=L'\cos\theta_1 \tag{3}$$

When supposing t is the growth time of the dendrite, L'' can also be expressed as

$$L''=\frac{(V_1\cos\theta_1-V_2\cos\theta_2)t}{\cos\theta_1}+L'\cos\left(\frac{\pi}{2}-\theta_1\right)=\frac{(V_1\cos\theta_1-V_2\cos\theta_2)t}{\cos\theta_1}+L'\sin\theta_1 \tag{4}$$

By combining Eq. (3) and Eq. (4), it yields

$$L'\cos\theta_1=\frac{(V_1\cos\theta_1-V_2\cos\theta_2)t}{\cos\theta_1}+L'\sin\theta_1 \tag{5}$$

Substituting Eq. (2) into Eq. (5) gives

$$L=\left[\frac{(V_1\cos\theta_1-V_2\cos\theta_2)}{\cos^2\theta_1-1/2\sin2\theta_1}+V_2(\sin\theta_2-\cos\theta_2\cdot\tan\theta_1)\right]t \tag{6}$$

To simplify the above equation, M is defined as

$$M=\frac{(V_1\cos\theta_1-V_2\cos\theta_2)}{\cos^2\theta_1-1/2\sin(2\theta_1)}+V_2(\sin\theta_2-\cos\theta_2\cdot\tan\theta_1) \tag{7}$$

Equation (6) becomes

$$t=L/M \tag{8}$$

It can be seen from Eq. (8) that there is a critical situation determined by the value of M, depending on the ratio of V_1 and V_2.

The critical situation is discussed. When M=0, there is

$$V_1/V_2=[\cos\theta_2-(\sin\theta_2-\cos\theta_2\cdot\tan\theta_1)\cdot(\cos^2\theta_1-1/2\sin(2\theta_1))]/\cos\theta_1 \tag{9}$$

For comparison with the W−C model, f_{SDAB} is defined, following the format of the W−C model in Eq. (1):

$$\frac{V_1}{V_2}=\frac{\cos\theta_2}{\cos\theta_1}[1-(\tan\theta_2-\tan\theta_1)\cdot(\cos\theta_1-\sin\theta_1)\cos\theta_1]=f_{SDAB}(\theta_1,\theta_2) \quad (10)$$

By comparing Eq. (10) and the W−C model, the difference of SDAB model and the W−C model lies in a factor which is smaller than 1, defined as

$$f_{SDAB}(\theta_1,\theta_2)=f_{W-C}(\theta_1,\theta_2)[1-(\tan\theta_2-\tan\theta_1)\cdot(\cos\theta_1-\sin\theta_1)\cos\theta_1]<f_{W-C}(\theta_1,\theta_2) \quad (11)$$

As can be seen in Eq. (11), it has three possibilities in the competitive growth when considering the blocking of the secondary arms:

(1) When $V_1/V_2>f_{SDAD}(\theta_1, \theta_2)$, and $M>0$, the secondary dendrite arm of FO grain blocks UO. In this case, smaller misorientation between grain boundary increases the possibility of the elimination of the UO grains, indicating that the occurrence of the secondary arms speeds up the elimination of the UO grains, maybe attributed to the enrichment of the solute by the growth of the secondary arms.

(2) When $V_1/V_2>f_{SDAD}(\theta_1, \theta_2)$ and $M=0$, the elimination would never happen, which cannot be predicted by the W−C model.

(3) When $V_1/V_2>f_{SDAD}(\theta_1, \theta_2)$ and $M<0$, the deviation of the W−C model would happen. Once the velocity of V_1 is not large enough, the UO grain has a possibility to avoid the elimination as observed in the experiment. For example, the farther the Grain G from Grain F, the faster the growth of tertiary dendrite arms, which eventually would develop into primary dendrite arms. If there is no dendrite, e.g. F4 blocking the primary dendrite arm of G grain at the grain boundary, Dendrite G_2_3 can surpass Dendrite F3 according to the relationship between Dendrite F3 and Dendrite G_2_3, i.e. $V_{F3}/V_{G\_2_3}=0.773<f_{SDAB}(\theta_F,\theta_G)=0.78$.

Table 3 gives the results of the convergence competition by the W−C model and SDAB model proposed. If the competition between Grains B and C is judged according to the W−C model, the C3 and C4 dendrites would surpass the growth of the B dendrites, but the experimental observations are consistent with the SDAB model. Likewise, the competition between Grains F and G are in-line with the SDAB model rather than the W−C model. It can be seen that the SDAB model reduces the critical value of the converging competitive speed ratio, which is closer to the experimental results than W−C model by considering the effect of side branches during competitive growth.

5 Conclusions

(1) In the process of competitive growth, the FO grain and the UO grain did not simply follow the W−C model or even maintain the converging or diverging growth. The primary dendrite arm spacing can be adjusted by the spontaneous development of tertiary dendrite arms inside the grain, and competitive growth may occur between the secondary dendrite arms and the tertiary dendrite arms.

(2) When grain growth was inhibited, a new growth path was established through self-regulation and transformation of the competitive relationship.

(3) CDT (converging-to-diverging transition) or DCT (diverging-to-converging transition) can occur through the deflection of the growth direction.

Table 3 Comparison of converging competition result predicted by W−C model and "secondary dendrite arm blocking model" (SDAB model)

Competition between Grain B (14°) and Grain C (21°)						
V_B/V_{C1}	V_B/V_{C2}	V_B/V_{C3}	V_B/V_{C4}	$f_{W-C}(\theta_B,\theta_C)$	$f_{SDAB}(\theta_B,\theta_C)$	Prediction
1.19	1.19	0.93	0.95	0.96	0.87	C3 and C4 blocked by secondary arms of B
Competition between Grain F (20°) and Grain G (31.5°)						
V_{F4}/V_G	$V_{F4}/V_{G\_1_3}$	$V_{F4}/V_{G\_2_3}$	$f_{W-C}(\theta_F,\theta_G)$	$f_{SDAB}(\theta_F,\theta_G)$	Prediction	
1.19	0.94	0.86	0.91	0.78	G_2_3 blocked by secondary arms of F4	

(4) Both converging competitive growth and diverging competitive growth are likely to form solute grooves at the solidification front and to generate CET (columnar-to-equiaxed transition).

(5) Especially the side branches have strong effect on the result of the competitive growth. Based on the experiments, “secondary dendrite arm blocking model” (SDAB model) considering the blocking effect of side branches was established. The SDAB model reduces the critical value of the converging competitive speed ratio, which is in closer agreement to the experimental results than the W−C model.

CRediT authorship contribution statement

Fa-guo LI: Investigation, Methodology, Writing − Original draft & editing, Funding acquisition; **Lian ZHOU:** Data curation, Writing − Review & editing; **Yu XIE:** Formal analysis, Writing − Review & editing; **Jiao ZHANG:** Conceptualization, Resources, Funding acquisition; **Mike DODGE:** Writing − Review & editing; **Fu-cheng YIN:** Writing – Review; **Bao-de SUN:** Supervision, Project administration.

Declaration of competing interest

The authors declare that they have no known competing financial interests or personal relationships that could have appeared to influence the work reported in this paper.

Acknowledgments

This work was supported by the Natural Science Foundation of Hunan Province, China (No. 2021JJ30672), the Science and Technology Project of Education Department of Hunan Province, China (No. 22A0100), the National Natural Science Foundation of China (No. 51627802), and Xiangtan University Scientific Research Start-up Fund. Thanks are also given to the BL13WB1 of Shanghai Synchrotron Radiation Facility (Shanghai, China) for providing the beam time and experimental assistance.

References

[1] POLLOCK T M. Alloy design for aircraft engines [J]. Nature Materials, 2016, 15: 809−815.

[2] YANG Wan-peng, LI Jia-rong, LIU Shi-zhong, SHI Zhen-xue, ZHAO Jin-qian, WANG Xiao-guang. Orientation dependence of transverse tensile properties of nickel-based third generation single crystal superalloy DD9 from 760 to 1100 °C [J]. Transactions of Nonferrous Metals Society of China, 2019, 29(3): 558−568.

[3] DAI H J, D'SOUZA N, DONG H B. Grain selection in spiral selectors during investment casting of single-crystal turbine blades: Part I. experimental investigation [J]. Metallurgical and Materials Transactions A, 2011, 42: 3430−3438.

[4] HALLENSLEBEN P, SCHAAR H, THOME P, JÖNS N, JAFARIZADEH A, STEINBACH I, EGGELER G, FRENZEL J. On the evolution of cast microstructures during processing of single crystal Ni-base superalloys using a Bridgman seed technique [J]. Materials & Design, 2017, 128: 98−111.

[5] LI Jun-jie, WANG Zhi-jun, WANG Ya-qin, WANG Jin-cheng. Phase-field study of competitive dendritic growth of converging grains during directional solidification [J]. Acta Materialia, 2012, 60: 1478−1493.

[6] WALTON D, CHALMERS B. The origin of the preferred orientation in the columnar zone of ingots [J]. Transactions of the AIME, 1959, 215: 447−457.

[7] ZHOU Y Z, VOLEK A, GREEN N R. Mechanism of competitive grain growth in directional solidification of a nickel-base superalloy [J]. Acta Materialia, 2008, 56: 2631−2637.

[8] TOURRET D, SONG Y, CLARKE A J, KARMA A. Grain growth competition during thin-sample directional solidification of dendritic microstructures: A phase-field study [J]. Acta Materialia, 2017, 122: 220−235.

[9] MENG X B, LU Q, ZHANG X L, LI J G, CHEN Z Q, WANG Y H, ZHOU Y Z, JIN T, SUN X F, HU Z Q. Mechanism of competitive growth during directional solidification of a nickel-base superalloy in a three-dimensional reference frame [J]. Acta Materialia, 2012, 60: 3965−3975.

[10] HU Song-song, LIU Lin, YANG Wen-chao, SUN De-jian, HUO Miao, HUANG Tai-wen, ZHANG Jun, SU Hai-jun, FU Heng-zhi. Formation of accumulated misorientation during directional solidification of Ni-based single-crystal superalloys [J]. Metallurgical and Materials Transactions A, 2019, 50: 1607−1610.

[11] GUO Chun-wen, LI Jun-jie, WANG Zhi-jun, WANG Jin-cheng. Non-uniplanar competitive growth of columnar dendritic grains during directional solidification in quasi-2D and 3D configurations [J]. Materials & Design, 2018, 151: 141−153.

[12] ESAKA H, SHINOZUKA K, TAMURA M. Analysis of single crystal casting process taking into account the shape of pigtail [J]. Materials Science & Engineering A, 2005, 413/414: 151−155.

[13] TOURRET D, KARMA A. Growth competition of columnar dendritic grains: A phase-field study [J]. Acta Materialia, 2015, 82: 64−83.

[14] DORARI E, JI K, GUILLEMOT G, GANDIN CH A, KARMA A. Growth competition between columnar dendritic grains – The role of microstructural length scales [J]. Acta Materialia, 2022, 223: 117395.

[15] GUO Chun-wen, LI Jun-jie, YU Hong-lei, WANG Zhi-jun, LIN Xin, WANG Jin-cheng. Branching-induced grain boundary evolution during directional solidification of columnar dendritic grains [J]. Acta Materialia, 2017, 136: 148−163.

[16] ZHOU Yi-zhou. Formation of stray grains during directional solidification of a nickel-based superalloy [J]. Scripta Materialia, 2011, 65(4): 281−284.

[17] WANG Yu-min, LI Shuang-ming, LIU Zhen-peng, YANG Bin, ZHONG Hong, XING Hui. Competitive growth of degenerate pattern and dendrites during directional solidification of a bicrystal metallic alloy [J]. Metallurgical and Materials Transactions A, 2019, 50: 4677−4685.
[18] XING Hui, JI Ming-yue, DONG Xiang-lei, WANG Yu-min, ZHANG Li-min, LI Shuang-ming. Growth competition between columnar dendrite and degenerate seaweed during directional solidification of alloys: Insights from multi-phase field simulations [J]. Materials & Design, 2020, 185: 108250.
[19] MENG X B, LI J G, JING C N, LIU J D, MA S Y, LIANG J J, ZHANG C W, WANG M, TANG B T, LIN T, CHEN J L, ZHANG X L, LI Q. Misorientation dependent thermal condition-solute field cooperative effect on competitive grain growth in the converging case during directional solidification of a nickel-base superalloy [J]. Journal of Materials Science & Technology, 2022, 96: 151−159.
[20] LI Fa-guo, DONG Qing, ZHANG Jiao, DAI Yong-bing, FU Ya-nan, XIE Hong-lan, YIN Fu-cheng, SUN Bao-de. In situ study on the columnar-equiaxed transition and anaxial columnar dendrite growth of Al−15wt.%Cu alloy by synchrotron radiography [J]. Transactions of Nonferrous Metals Society of China, 2014, 24(7): 2112−2116.
[21] LU Wen-quan, ZHANG Nai-fang, DING Zong-ye, HU Qiao-dan, LI Jian-guo. Recent progress on apparatus development and in situ observation of metal solidification processes via synchrotron radiation X-ray imaging: A review [J]. Transactions of Nonferrous Metals Society of China, 2022, 32(8): 2451−2479.
[22] CLOETENS P, BOLLER E, LUDWIG W, BARUCHEL J, SCHLENKER M. Absorption and phase imaging with synchrotron radiation [J]. Europhysics News, 2001, 32(2): 46−50.
[23] CHEN Rong-chang, LIU Ping, XIAO Ti-qiao, XU L X. X-ray imaging for non-destructive microstructure analysis at SSRF [J]. Advanced Materials, 2014, 26(46): 7688−7691.
[24] LI Fa-guo, ZHANG Jiao, DONG Qing, DAI Yong-bing, FU Ya-nan, XIE Hong-lan, MI J, YIN Fu-cheng, SUN Bao-de. In situ synchrotron X-ray studies of the coupled effects of thermal and solutal supercoolings on the instability of dendrite growth [J]. Materials Characterization, 2015, 109: 9−18.
[25] GANDIN CH A, ESHELMAN M, TRIVEDI R. Orientation dependence of primary dendrite spacing [J]. Metallurgical and Materials Transactions A, 1996, 27: 2727−2739.
[26] WANG Zhi-ping, WANG Jun-wei, ZHU Chang-sheng, FENG Li, XIAO Rong-zhen. Phase-field simulations of forced flow effect on dendritic growth perpendicular to flow [J]. Transactions of Nonferrous Metals Society of China, 2011, 21(3): 612−617.
[27] REINHART G, MANGELINCK-NOËL N, NGUYEN-THI H, SCHENK T, GASTALDI J, BILLIA B, PINO P, HÄRTWIG J, BARUCHEL J. Investigation of columnar-equiaxed transition and equiaxed growth of aluminium based alloys by X-ray radiography [J]. Materials Science and Engineering A, 2005, 413/414: 384−388.
[28] LI Fa-guo, YIN Fu-cheng, ZHANG Jiao, FU Ya-nan, SUN Bao-de. The effect of local thermo-solutal convection on dendrite fragments at variable cross section [J]. Materials Research Express, 2019, 6: 1165b6.
[29] BOGNO A, NGUYEN-THI H, REINHART G, BILLIA B, BARUCHEL J. Growth and interaction of dendritic equiaxed grains: In situ characterization by synchrotron X-ray radiography [J]. Acta Materialia, 2013, 61: 1303−1315.
[30] GANDIN CH A, RAPPAZ M. A coupled finite element−cellular automaton model for the prediction of dendritic grain structures in solidification processes [J]. Acta Metallurgica et Materialia, 1994, 42(7): 2233−2246.
[31] PINEAU A, GUILLEMOT G, TOURRET D, KARMA A, GANDIN CH A. Growth competition between columnar dendritic grains − Cellular automaton versus phase field modeling [J]. Acta Materialia, 2018, 155: 286−301.

Al−20%Cu 多晶粒竞争生长的原位观测及汇聚型枝晶淘汰模型构建

李发国[1]，周 莲[1]，谢 玉[2]，张 佼[3]，Mike DODGE[4]，尹付成[1]，孙宝德[3]

1. 湘潭大学 材料科学与工程学院 湖南省材料设计与制备技术重点实验室，湘潭 411105；
2. 宝山钢铁有限公司 中央研究院，上海 201900；
3. 上海交通大学 材料科学与工程学院，上海 200240；
4. TWI Ltd, Granta Park, Great Abington, Cambridge CB21 6AL, UK

摘 要：采用同步辐射成像技术研究 Al−20%Cu(质量分数)亚共晶合金的晶粒竞争生长动力学，并建立与实验结果相一致的数学模型。结果表明，对于发散型竞争生长，遵循“正常淘汰”规则。对于汇聚型竞争生长，成分过冷的作用加速非择优取向晶粒中一次枝晶臂的生长速度，导致非择优取向枝晶出现“异常淘汰”现象，淘汰择优取向枝晶。探讨汇聚型竞争生长的“正常淘汰”与“异常淘汰”之间的临界条件，建立枝晶生长速率、枝晶臂间距和枝晶倾斜角之间的数学关系，又称“二次枝晶臂阻挡模型”，可以快速预测晶界位相和淘汰类型。

关键词：竞争生长；同步辐射成像；定向凝固；数学模型；Al−Cu 合金

(Edited by Bing YANG)